Eur Biophys J (1992) 20:337–344

European Biophysics Journal

Annexin V membrane interaction: an electrostatic potential study

Andrej Karshikov [1], Robert Berendes [1], Alexander Burger [1], Adolfo Cavalié [2], Hans-Dieter Lux [2], and Robert Huber [1]

[1] Max-Planck Institut für Biochemie and [2] Max-Planck Institut für Psychiatrie, W-8033 Martinsried, Federal Republic of Germany

Received July 25, 1991 / Accepted in revised form October 23, 1991

Abstract. The possible role of electrostatic interactions for membrane binding and pore formation of annexin V has been analysed on the basis of a simple dielectric model. It is suggested that the binding of phospholipids to annexin V is regulated, at least initially, by the protein's electrostatic potential. The calculations show that a strong local gradient of the electrostatic potential exists at the membrane-protein interface and a membrane pore may be generated by electroporation. The observed specificity and regulation of ion conduction is suggested to reside in the protein part of the pore. On the basis of the three-dimensional structures of the protein and its hypothetical membrane complex, and electrophysiological measurements, a mechanical model of the transmembrane voltage regulation of the annexin's ion conduction properties is proposed.

Key words: Annexin V – Electrostatic interactions – Electroporation – Calcium channel

Introduction

Annexins form a large family of calcium and phospholipid binding proteins found in a variety of organisms and cell types. Annexin V (also named endonexin II or vascular anticoagulant α) is an intensively studied member of this family. This protein is very soluble in water and associates with membranes in a Ca^{2+} dependent manner (Schlaepfer et al. 1987; Andree et al. 1990). Membrane binding requires the presence of acidic phospholipids, such as phosphatidylserine (Schlaepfer et al. 1987). Once bound to the membrane, annexin V forms a calcium selective voltage-gated cation channel with prominent selectivity for Ca^{2+} ions (Rojas et al. 1990).

The determination of the molecular structure of water soluble annexin V as three-dimensional crystals (Huber et al. 1990a, b) and of phospholipid bound annexin as two-dimensional layers (Brisson et al. 1991; Mosser et al. 1991) provide a basis for a better understanding of the phenomena mentioned above. It has been found that the molecule of annexin V is folded into four domains arranged around a central axis with approximate two-fold symmetry which marks a hydrophilic region in the protein core. We associated this structure with the Ca^{2+} permeable channel (Huber et al. 1990a). Moreover, three calcium and two lanthanum binding sites have been identified. All these ions are bound to the convex face of the protein. This, along with other arguments summarized by Brisson et al. (1991), strongly suggest that this face is the membrane-protein interface. The central hydrophilic channel is normal to the membrane plane.

The adsorption of annexin V to a phospholipid monolayer increases the surface pressure (Berendes et al. unpublished results) indicating partial penetration of the protein into the membrane or rearrangement of the phospholipid layer by some other mechanism in the contact region. No experimental evidence of the detailed mode of annexin phospholipid binding is available but the structural similarity of the calcium binding loops of annexin V to phospholipase A_2 (Huber et al. 1990b) suggests similarities in phospholipid binding mode, i.e. Ca^{2+}-phosphoryl moiety coordination.

The accurate structural definition of the protein part contrasts the lack of information about the membrane structure as a basis for its ion permeability. We have suggested that binding of phospholipids to the protein and calcium ions may destabilize the membrane part (Brisson et al. 1991). It is also known that an external electric field may cause structural reorganization of the membrane, leading to reversible pore formation (electroporation) (Sugar and Neumann 1984; Sugar et al. 1987; Schlaepfer et al. 1987). Neumann (1988) has analysed the parameters determining the pore formation and has shown that pore opening occurs if a threshold transmembrane voltage V_t is achieved. The value of V_t depends on the duration of the applied external electric field: for short pulses (duration about 10 μs) V_t is between 0.5 and 1 volts, for longer pulses ($\geq$0.1 ms) it is reduced to 0.2–0.5 volts.

Offprint requests to: R. Huber

In this paper we analyse the role of electrostatic interactions in membrane binding of annexin V and their effect on the membrane, using a simple dielectric model: the membrane and the protein were treated as a medium with a low dielectric constant surrounded by the solvent as a medium of high permittivity. The spatial distribution of the protein electrostatic potential was calculated for this system using the finite difference algorithm for the numerical solution of the Poisson-Boltzmann equations developed by Honig and co-workers (Klapper et al. 1986; Sharp and Honig 1990).

The calculations show that electrostatic interactions play an essential role in membrane-protein binding: The highest three maxima of the electrostatic potential in the membrane-protein interface were found in the vicinity of the three protruding calcium-binding loops of the protein. They probably constitute the putative anionic phospholipid binding areas. A strong gradient of the electrostatic potential was obtained across the membrane. A large area of the protein-membrane interface, including also the La^{3+} binding sites, was found to have a potential value equal to or more negative than -0.2 volts, suggesting the possibility of electroporation. The analysis of the salt bridges in the central hydrophilic protein cavity showed that small changes of the conformations of the participating groups may lead to a widening of this cavity thereby altering the ion conduction properties. On this basis we present a mechanical model of the voltage-gated channel and correlate its properties with electrophysiological data.

Method of calculations

The calculations of the electrostatic interactions were based on a simple macroscopic dielectric model. The scheme of the model is shown in Fig. 1. The protein and the membrane moieties were represented as a continuum with low dielectric constant surrounded by the solvent with $\varepsilon = 78$. There are a variety of investigations suggesting values of the protein dielectric constant between 2 and 50 (Warshel et al. 1984; Gilson and Honig 1988; Nakamura et al. 1988). The theoretical investigations made by Gilson and Honig (1986) give a value between 2.5 and 4. The higher values of ε mentioned in the literature are effective values and are often extracted from effects such as the change of pK of the titratable groups (Sternberg et al. 1987; Russell et al. 1987), or reduction of the energy of electrostatic interactions in respect to vacuum. In fact, a high effective dielectric constant may be obtained by models using low permittivity for the protein (dielectric cavity models) and it reflects the screening effect of the shape of the solvent/protein boundary (Jayaram et al. 1989). Therefore, a value between 2 and 4 is appropriate for the low dielectric moiety in our model.

The membrane of thickness 40 Å is in contact with the convex face of the protein by direct interaction of the calcium ions with the phosphoryl moiety of the phospholipid. Accordingly, the proximal leaflet of the membrane was chosen to lie in the plane defined by the coordinates of the three calcium ions. Thus, in our model complex the protein molecule penetrates the membrane by 6 Å mainly with the hydrophobic residues *Ala* 103, *Ala* 262, and *Leu* 31 which protrude from the calcium-binding loops and may interact with the hydrocarbon part of the membrane.

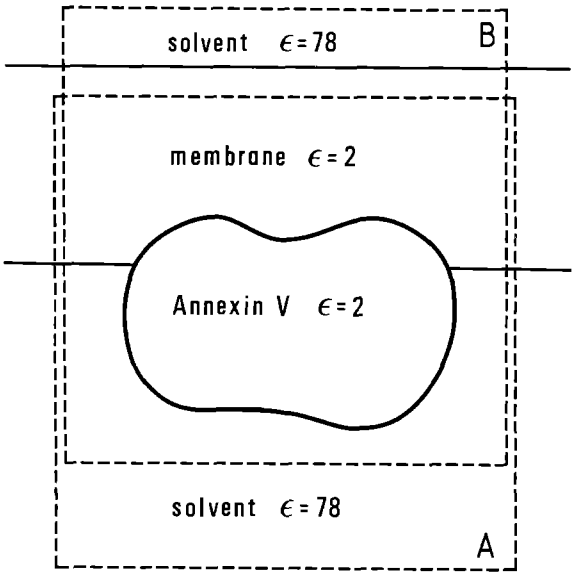

Fig. 1. Scheme of the dielectric model used in the calculations of the electrostatic potential. The protein molecule and the membrane are assumed to be media with low dielectric constant ($\varepsilon = 2$) surrounded by the solvent ($\varepsilon = 78$). The calculations of the electrostatic potential in the protein-membrane interface region have been carried out in box A by including the whole protein and the proximal part of the membrane. The final calculations have been made in a box $97 \times 97 \times 97$ Å and grid 1.5 Å. The calculations of the electrostatic potential in the membrane have been performed in box B which also includes the distal side of the membrane (final box size $92 \times 92 \times 92$ Å, grid 1.4)

The electrostatic potential was calculated on the basis of the numerical solution of the Poisson-Boltzmann equations using the finite difference algorithm developed by Honig and co-workers (Klapper et al. 1986; Sharp and Honig 1990). The charge constellation of the proteins was defined only by the charges carried by the ionizable groups and the three calcium ions. The calculations were performed for an ionic strength of 0.1 at pH 7.0. At this pH all charged groups have positive or negative charges of unity except the histidines and the amino-terminus. The intrinsic pK of histidines is about 6.3 but may change owing to the environment in the protein (Sternberg et al. 1987; Delepierre et al. 1987; Spassov et al. 1989; Karshikov et al. 1989). We therefore calculated the pK, and hence the charges of these groups using the fast computational procedure described by Karshikov et al. (1989). The charge values used in the calculations are listed in Table 1.

Two runs of finite difference calculations were carried out. The purpose of the first one was to localize the maxima of the positive electrostatic potential as a possible location of the anionic phospholipid headgroups. The computations were performed in a box including the protein molecule and the proximal leaflet of the membrane. In this case the electrostatic potential on the protein-membrane interface was calculated. This inter-

Table 1. Charge values used in the calculations of the electrostatic potential

Atom type[a]	Residue	Charge[b]
N	N-trm	0.83
O	C-trm	−0.5
OXT	C-trm	−0.5
NZ	*lys*	1.0
NH1	*arg*	0.5
NH2	*arg*	0.5
OE1	*glu*	−0.5
OE2	*glu*	−0.5
OD1	*asp*	−0.5
OD2	*asp*	−0.5
ND1	*His* 98	0.05
NE2	*His* 98	0.05
ND1	*His* 205	0.25
NE2	*His* 205	0.25
ND1	*His* 267	0.13
NE2	*His* 267	0.13
CA	Calcium	2.0

[a] Atom types are given according to the Brookhaven Protein Data Bank (Bernstein et al. 1977)
[b] The charge values are given in protonic units

face was determined by the plane of the proximal membrane leaflet and the surface of the protein atoms accessible to a counteratom with radius of 3 Å (the approximate radius of a phospholipid headgroup).

The second run included the protein molecule, the entire membrane, and the solvent behind the distal leaflet of the membrane (see Fig. 1). The charges of the anionic phospholipid headgroups obtained from the first run were also included in the calculations. Coulombic boundary conditions (Klapper et al. 1986) were applied for both runs. Each run was repeated using two step focussing calculations (Gilson et al. 1987).

The calculations were carried out for two values of the low dielectric constant, $\varepsilon = 2$ and $\varepsilon = 4$, and for two values of the membrane thickness of 36 Å and 40 Å. Essentially similar results were obtained. For further analysis $\varepsilon = 2$ and a membrane thickness of 40 Å were chosen. The finite difference calculations were performed with the program package DELPHI (Klapper et al. 1986; Gilson et al. 1985). Minor changes of the program were made which allow a representation of the electrostatic potential using FRODO (Jones 1978) graphic facilities.

Results and discussion

The main goal of our study was to analyse the role of electrostatics in annexin V – membrane interactions. It is known that this protein binds to membranes containing anionic phospholipids (Schlaepfer et al. 1987; Andree et al. 1990). The presence of these charged groups in the membrane-protein contact region may change the potential within the membrane, so that we first attempted to determine their positions.

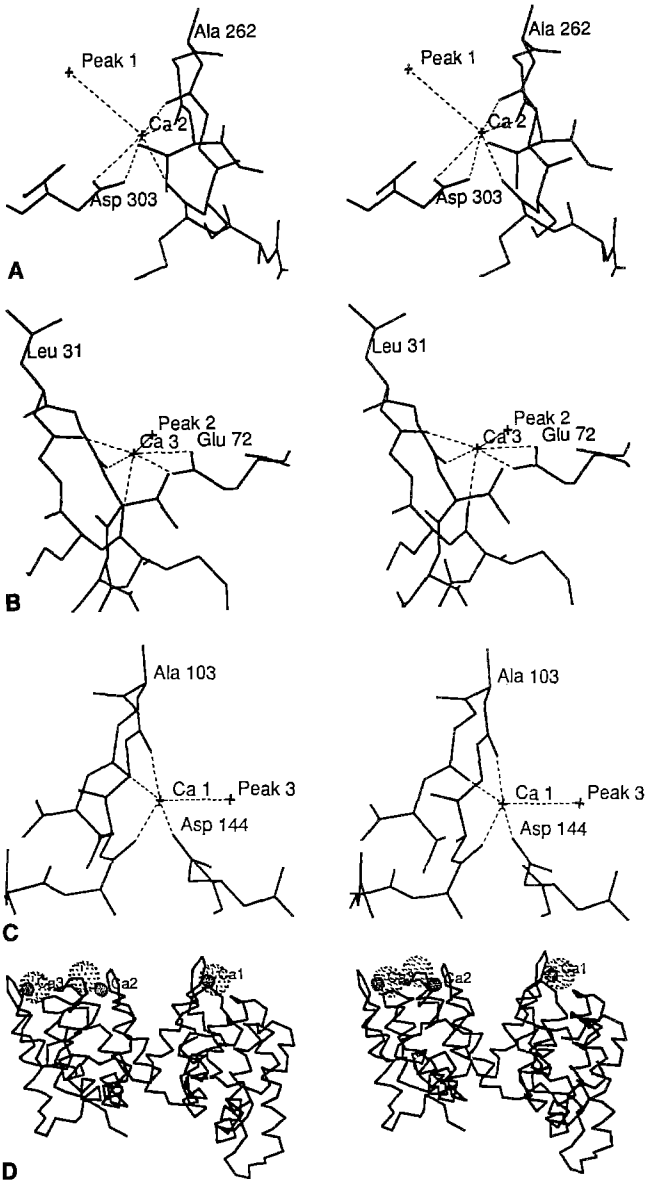

Fig. 2A–D. Locations of the phospholipid negative charges determined according to the maxima of the electrostatic potential in the protein-membrane interface. **A** The global electrostatic potential maximum (peak 1) in the vicinity of Ca_2^{2+}; **B** and **C** The positions of the second (peak 2) and the third (peak 3) maxima are close to Ca_3^{2+} and Ca_1^{2+} respectively; **D** stereo view of the main chain folding of annexin V with the Ca^{2+} binding sites (little dotted spheres) and the putative location of the negatively charged phospholipid headgroups (large dotted spheres)

Binding of phospolipids to annexin V

The search of the probable positions of the membrane charges was made on the basis of the electrostatic interactions. The positions of the maxima of the electrostatic potential on the membrane-protein contact surface were assumed to be the locations of the negatively charged phospholipids. The global, second and third maxima are situated close to Ca_2^{2+}, Ca_3^{2+}, and Ca_1^{2+} respectively, as shown in Fig. 2. These positions have been suggested as phospholipid binding sites (also on the basis of structural considerations (Huber et al. 1990b)) and are assumed to

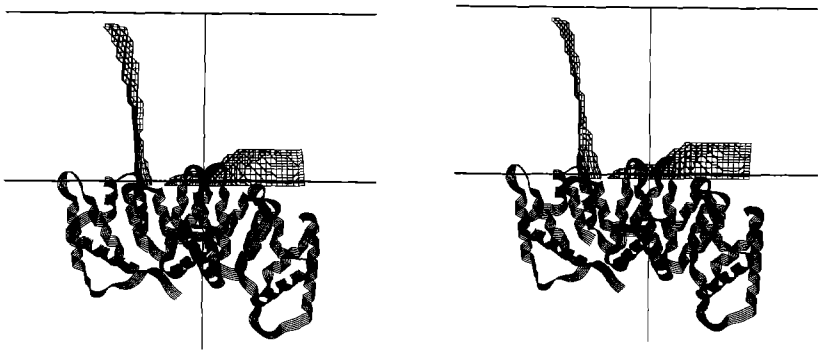

Fig. 3. Stereo view of the zero equipotential surface within the membrane. The space above domains I and IV (left hand side, see the scheme in the lower part of Fig. 4) is characterized by negative potential. Above domains II and III the potential disappears close to the protein-membrane interface (right hand side). The axis normal to the membrane marks the hydrophilic region in the protein core

present the anionic phospholipid binding sites for the following calculations.

A model for annexin membrane interaction

Calculations of the electrostatic potential in the bilayer (box B in Fig. 1) were performed by including the three negatively charged phospholipid groups. The coordinates of these charges correspond to the three highest maxima of the electrostatic potential in the membrane protein interface as described above (see Fig. 2). The distribution of the electrostatic potential in the membrane space is characterized by a strong asymmetry (Fig. 3). In the region adjacent to the module (II, III) (right hand side in Fig. 3) the electrostatic potential disappears close to the membrane-protein interface. The space adjacent to the module (I, IV), however, is characterized by a negative electrostatic potential, which reaches the distal leaflet of the membrane with a maximal value of 0.01 V. A large patch of negative electrostatic potential equal to or stronger than -0.2 V is observed at the protein-membrane interface, which covers almost all of domain I and includes the two La^{3+} binding sites (Fig. 4). A smaller patch is seen on the protein-membrane surface between the domains II and III.

It is known that an external electric field can invoke distortion of the membrane or formation of a membrane pore (Sugar and Neumann 1984; Sugar et al. 1987; Neumann 1988). Neumann (1988) has shown that a voltage of 0.2 to 0.5 V is sufficient if the external electric field acts on the membrane for more than 0.1 ms. The electrostatic field calculated above reaches these values and may therefore cause structural changes of the membrane similar to those in electroporation experiments. The distortion of the membrane area by annexin V binding is reflected by phospholipid monolayer experiments showing a substantial increase of the surface pressure (Berendes et al. unpublished results). Hence, we suggest that the specific calcium phospholipid interactions, which may be similar to those in phospholipase A_2, and the non-specific effects of the protein electrostatic field lead to local membrane reorganization and permeability change.

The La^{3+} binding sites are situated at the bottom of the penetrable part of the membrane (the pore) in the region of the strongest potential (Fig. 4). They may represent intermediate binding sites for Ca^{2+} in transit

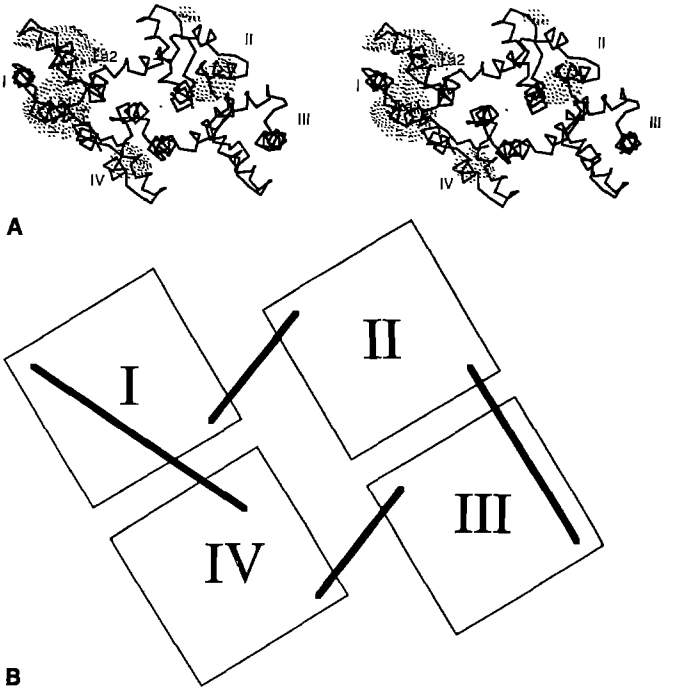

Fig. 4 A, B. Stereo view of the main chain folding of annexin V perpendicular to the membrane plane. The dotted surface embraces the protein-membrane interface region with electrostatic potential equal to or stronger than -0.2 V. The calculations were carried out in the presence of Ca_1^{2+}, Ca_2^{2+}, Ca_3^{2+} and the charges of the three negative phospholipid head groups. The Roman numbers indicate the four domains of the protein as shown in the scheme in **B**

through the channel. If occupied by La^{3+} ion flow may be inhibited: For example, 100 μM La^{3+} inhibits the Ca^{2+} current through annexin V (Berendes, unpublished results), supporting a competition between La^{3+} and Ca^{2+} for the intermediate binding site.

Model of the voltage gated ion channel

The proposed model of the annexin V – membrane interactions suggests that specificity and regulation of the ion conduction channel reside in the protein part. The analysis of kinetic data obtained by single channel recording (the experimental details will be presented elsewhere) showed that there are at least two open and two close mean times which exhibit a strong voltage dependence (Fig. 5). The existence of two mean life times implies two

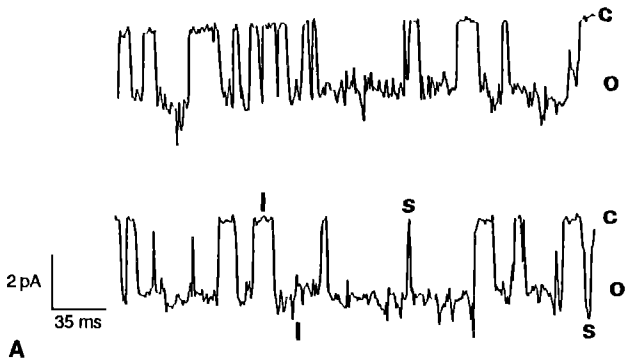

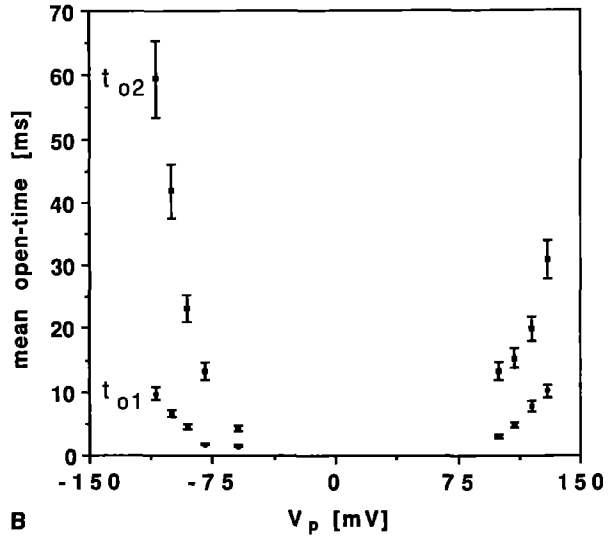

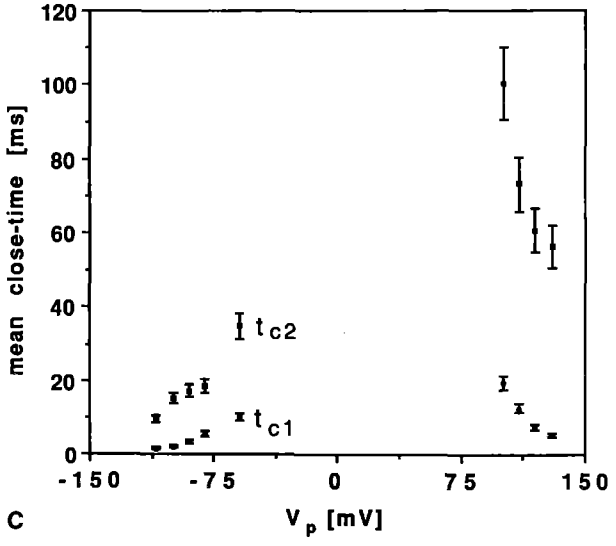

Fig. 5A–C. Voltage-gated channel kinetics. **A** Steady-state recordings of single channel activity at a pipette potential $V_p = -100$ mV; o: open state, **C** close state, l: characteristic long (open or closed) period, s: characteristic short, burst-like, (*open and closed*) period. **B** Mean open life times, τ_{O_1} and τ_{O_2}, and **C** mean close times, τ_{C_1} and τ_{C_2}, of recombinant annexin V versus pipette potential. Methods: liposomes were formed by the freeze-thaw method (Kasahara and Hinckle 1977) with phosphatidylethanolamine/phosphatidylserine at a weight ratio of 7 : 3. Prior to the experiments, annexin V was added to the liposome suspension to a concentration of 8 μM. This preparation was stored. Before use it was further diluted 500 fold.

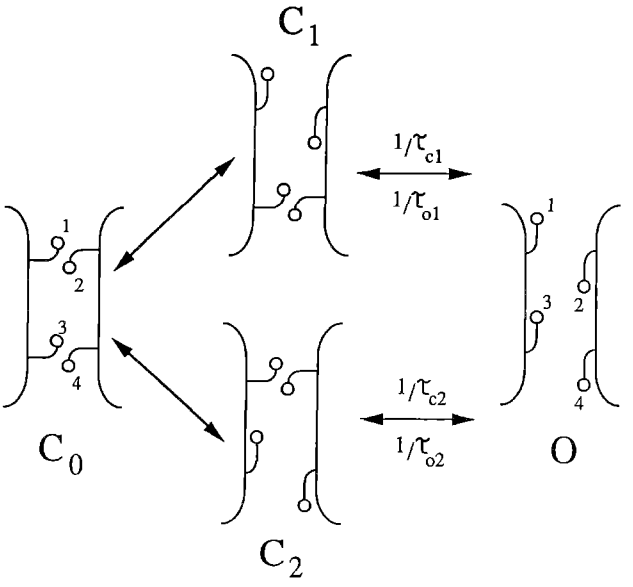

Fig. 6. Mechanical model of the voltage gated annexin V channel. According to the molecular structure of the central pore (see Fig. 8), an exemplary assignment of the gating charged groups may be the following: 1 – *Arg* 271, 2 – *Glu* 112, 3 – *Arg* 117, and 4 – *Arg* 276

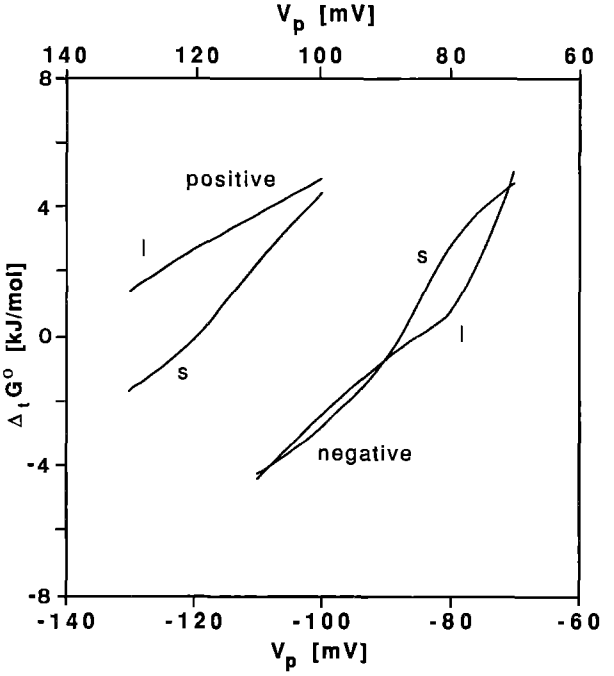

Fig. 7. Voltage dependence of the standard Gibbs free energy of the transitions between closed and open channel: s – short open and close life times, l – long open and close life times. V_p means peptide potential

The measurements were done in the "inside-out" recording mode of the patch-clamp technique (Hamill et al. 1981). In this configuration, the incorporated annexin V is in the lipid layer facing the pipette solution. Symmetrical solutions were used and contained (in mM): 1 $CaCl_2$, 10 tetraethylammonium-HEPES, pH 6.5. The membrane potential across the bilayer was changed by clamping the V_p with respect to the bath. A positive current is defined as net cation flow from the pipette into the bath. The currents were filtered at 3–4 kHz and digitized at 1 kHz. Data were analysed off-line with the program AUTESP developed by H Zucker (Dept. Neurophysiology, Max Planck Institute of Psychiatry, Martinsried, Germany)

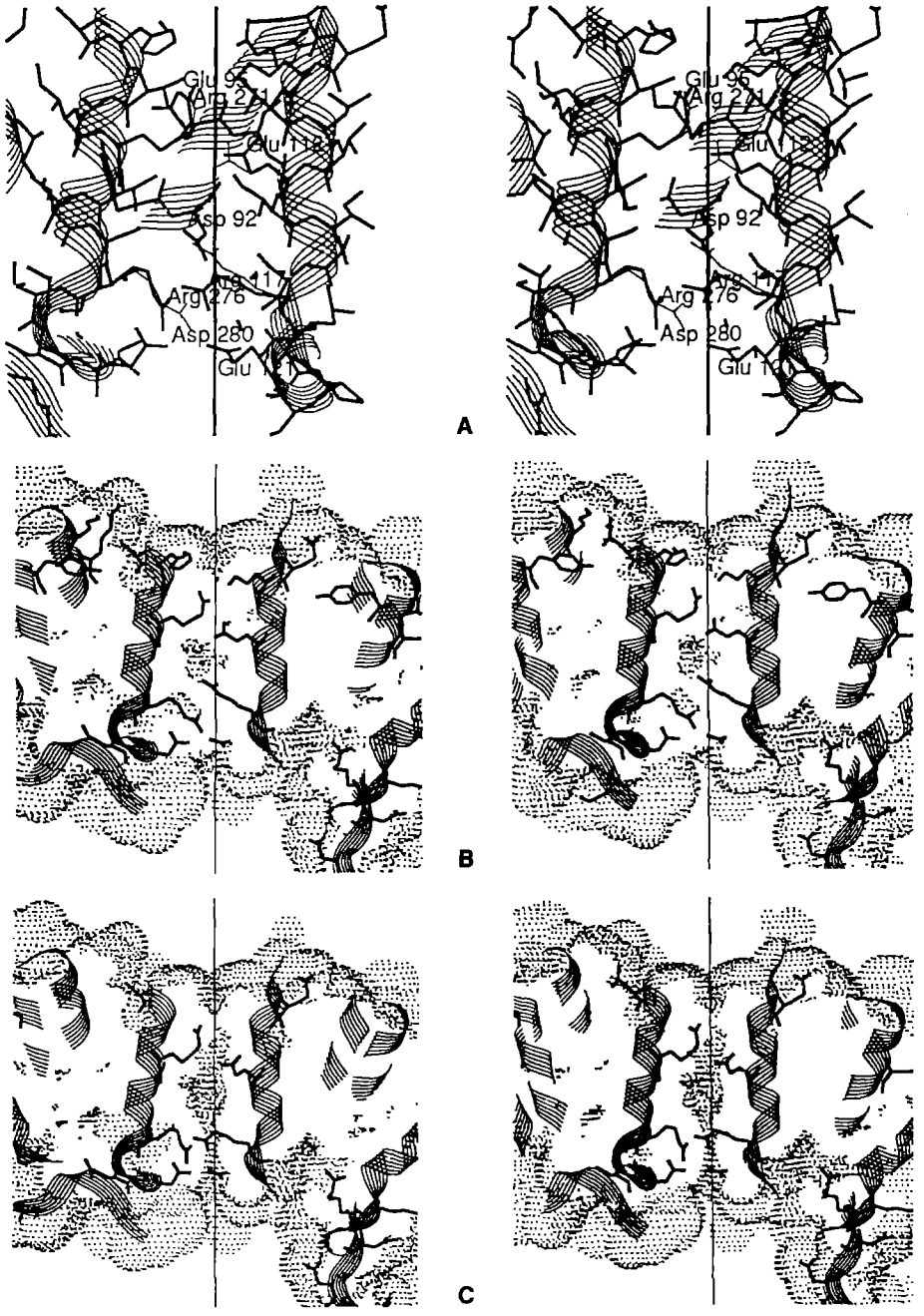

Fig. 8A–C. Stereo view of the central protein cavity. The main chain of the protein is represented by ribbon. **A** The observed conformations of the side chains are given by thin lines. The suggested model conformation for the open state of the channel is shown by thick lines. **B** The central cavity observed in crystals and supposed to be the closed state. The dotted surfaces represent the accessibility of the protein atoms to a counter atom with radius 1 Å. The central cavity is not accessible to external atoms owing to *Arg* 271 and *Glu* 112 at the side, and to both arginines 117 and 276 at the other side. **C** Hypothetical conformations of the charged groups (labeled in a) allowing opening of the central cavity

conformational transitions leading to opening/closing of the channel. A possible model in agreement with the structural and kinetic data is shown in Fig. 6 in which the existence of one open and at least two different closed states are assumed. The open-closed transitions are regulated by independent opening/closing of two gates. Two closed gates correspond to the state designated as C_0 in Fig. 6. The closed states C_1 and C_2 have only one gate closed while the other is open. The single channel recordings show periods with long openings and closings well separated from burst-like periods with short closings and openings in the current records of annexin V (Fig. 5a). These two sets of mean open and mean close life times are ascribed in the model to the transitions from the states C_1 and C_2 to state 0 (open channel). The transitions C_0-C_1 and C_0-C_2 are silent within our single channel measurements. The transitions to the open state can be described as follows:

$$C_1 \underset{1/\tau_{O_1}}{\overset{1/\tau_{C_1}}{\rightleftharpoons}} O \quad \text{and} \quad C_2 \underset{1/\tau_{O_2}}{\overset{1/\tau_{C_2}}{\rightleftharpoons}} O,$$

where τ_{O_1} and τ_{C_1} are the short open and close mean life time and τ_{O_2} and τ_{C_2} are the corresponding long mean life times. The rate constants of the above transitions are the reciprocal values of the mean life times (Colquhoun and Hawkes 1981). From the equilibrium constants of the above transitions, $K_1 = \tau_{O_1}/\tau_{C_1}$ and $K_2 = \tau_{O_2}/\tau_{C_2}$, the corresponding standard Gibbs free energies $\Delta_t G_1^0 = -RT \ln(K_1)$ and $\Delta_t G_2^0 = -RT \ln(K_2)$ can be obtained. In Fig. 7, the voltage dependence of $\Delta_t G_1^0$ and $\Delta_t G_2^0$ i

shown. With the increase of the holding potential in both directions the opened state is increasingly favoured over the closed state indicating that charged groups or equivalent dipoles participate in the gating process.

We have ascribed the gating properties to the protein and suggested that the central pore in annexin V is the ion channel. Applied external voltage may cause module motion as seen when the $P6_3$ and R3 crystal structures (Huber et al. 1990a, b) are compared. It may also induce rearrangement of the charged amino acid residues surrounding the pore, which is an incision between modules (I, IV) and (II, III). The funnel shaped pore is formed by four α-helices and is widely open at the upper end, where it is in contact with the membrane and constricted at the opposite end. It is formed by a large cavity (Fig. 8) confined between two ionic clusters, which we associate with the two gates from the mechanical model. Gate 1 is formed by the salt bridge *Arg* 271 – *Glu* 112 across the protein pore and the closely situated *Glu* 95. The second gate (gate 2) is constituted by *Arg* 117 (forming a salt bridge with *Glu* 95) and *Arg* 271 (engaged in strong ionic interactions with *Glu* 121 and *Asp* 280, see Fig. 8a). The conformation of these groups as observed in the X-ray structure supposedly corresponds to the closed state C_0 (both gates closed) of the channel (see Fig. 8b). It is worth noting that these residues are conserved in all known sequences of annexins except *Glu* 95 and 121 which may also be glutamines. The opening of gate 1 may proceed as follows: *Glu* 95 is in close proximity to *Arg* 271 and an appropriate candidate for a salt bridge. Thus, *Arg* 271 may form a new salt bridge with this group thereby breaking the salt bridge with *Glu* 112, which becomes accessible to the solvent and may depart from the ionic cluster. A similar rearrangement could open gate 2: *Glu* 121 may form a salt bridge with *Arg* 117, breaking its salt bridge with *Arg* 276. This exchange is accompanied with minor conformational changes of *Arg* 117 and *Arg* 276; the latter then approaches *Asp* 280 more closely. This change, possibly stimulated by the presence of the calcium ion, may be facilitated by the electrostatic repulsion of the charges of the two arginines.

A possible conformation of the gating groups in state 0 of the channel is shown in Fig. 8c. It is seen that drastic conformational changes of the side chains of these groups are not necessary to open the protein cavity. The main effect of this rearrangement is the exchange of the salt bridge partners of two groups: *Arg* 217 – *Glu* 112 to *Arg* 217 – *Glu* 95 and *Glu* 121 – *Arg* 276 to *Glu* 121 – *Arg* 117. In state 0 the charges of the participating groups remain in similar and favorable electrostatic environments, which suggests that the opening/closing of the gates is not accompanied by large changes of the electrostatic free energy. This conclusion is in accord with the measured values of ΔG, which do not exceed 1.5 kcal/mol (see Fig. 7). These conformational changes may be coupled with the observed collective "hinged domain motion" of the protein (Huber et al. 1990b); the calcium rich structure shows a widening of the central protein pore, which suggests an enhancement of the flexibility of the charged groups in this region. Both transitions are energetically equivalent at negative voltages, but different at positive voltages. This asymmetry results from the asymmetry of the protein and its charge distribution. We are not able, however, to assign the two mean life times observed to the two gates proposed. We approach this and other questions by site specific mutagenesis and functional and structural studies of the mutants.

References

Andree HAM, Reutelingsperger CPM, Hauptmann R, Hemker HC, Hermens WTh, Willems GM (1990) Binding of vascular anticoagulant α (VACα) to planar phospholipid bilayer. J Biol Chem 265:4923–4928

Bernstein FC, Koetzle TF, Williams GJB, Meyer EF jr., Brice MD, Rodgers JR, Kennard O, Shimanuochi T, Tasumi M (1977) The protein data bank: a computer based archival file for macromolecular structures. J Mol Biol 112:353–342

Brisson A, Mosser G, Huber R (1991) Structure of soluble and membrane-bound annexin V. J Mol Biol 220: in press

Colquhoun D, Hawkes AG (1981) On the stochastic properties of single ion channels. Proc R Soc London B112:205–235

Delepierre M, Dobson CM, Karplus M, Poulsen FM, States DJ, Wedin RE (1987) Electrostatic effects and hydrogen exchange in proteins. The pH dependence of exchange rate in lysozyme. J Mol Biol 197:111–130

Gilson MK, Honig BH (1986) The dielectric constant of a folded protein. Biopolymers 25:2097–2119

Gilson MK, Honig BH (1988) Energetics of charge-charge interaction in proteins. Proteins: Structure, Function, Genet 3:32–52

Gilson MK, Rashin A, Fine R, Honig B (1985) On the calculation of electrostatic interactions in proteins. J Mol Biol 183:503–516

Gilson MK, Sharp KA, Honig BH (1987) Calculations of electrostatic potential of molecules in solution; method and error assessment. J Comp Chem 9:237–335

Hamill OP, Marty A, Neher E, Sakmann B, Sigworth FJ (1981) Improved patch-clamp techniques for high-resolution current recording from cell and cell-free membranes. Pflügers Arch 391:85–100

Huber R, Schneider M, Mayr I, Römisch J, Paques E-P (1990a) The calcium binding sites in human annexin V by crystal structure analysis at 2.0 Å resolution. Implications for membrane binding and calcium channel activity. FEBS Lett 275:15–21

Huber R, Römisch J, Paques E-P (1990b) The crystal and molecular structure of human annexin V, an anticoagulant calcium, membrane binding protein. EMBO J 9:3867–3874

Jayaram B, Sharp KA, Honig B (1989) The electrostatic potential of B-DNA. Biopolymers 28:975–993

Jones A (1978) A graphic model building and refinement system for macromolecules. J Appl Crystallogr 11:268–272

Karshikov A, Engh R, Bode W, Atanasov B (1989) Electrostatic interactions in proteins: calculations of the electrostatic term of free energy and the electrostatic potential field. Eur Biophys J 17:287–297

Kasahara M, Hinckle PC (1977) Reconstitution and purification of the D-glucose transporter from human erythrocytes. J Biol Chem 252:7384–7390

Klapper I, Hagstrom R, Fine R, Sharp K, Honig B (1986) Focussing of electric field in the active site of Cu-Zn superoxide dismutase: Effect of ionic strength and aminoacid modification. Proteins: Structure, Function, Genet 1:47–59

Mosser G, Ravanat C, Freissinet J-M, Brisson A (1991) Sub-domain structure of lipid-bound annexin V resolved by image analysis. J Mol Biol 217:241–245

Nakamura H, Sakamoto T, Wada A (1988) A theoretical study of dielectric constant of proteins. Protein Eng 2:177–183

Neumann E (1988) The electroporation hysteresis. Ferroelectrics 86:325–333

Rojas E, Pollard HB, Haigler HT, Parra C, Burns L (1990) Calcium-activated endonexin II forms calcium channel across acidic

phospholipid bilayer membranes. J Biol Chem 256:21207–21215

Russell ST, Thomas PG, Fersht AR (1987) Electrostatic effects on modification of charged groups in the active site cleft of subtilisin by protein engineering. J Mol Biol 193:803–813

Schlaepfer DD, Mehlman T, Burgess WH, Haigler HT (1987) Structural and functional characterization of endonexin II, a calcium- and phospholipid binding protein. Proc Natl Acad Sci USA 84:6078–6082

Sharp KA, Honig B (1990) Electrostatic interactions in macromolecules: Theory and applications. Ann Rev Biophys Chem 19:301–332

Spassov VZ, Karshikov AD, Atanasov BP (1989) Electrostatic interactions in proteins. A theoretical analysis of lysozyme ionization. Biochim Biophys Acta 999:1–6

Sternberg MJE, Hayes FRF, Russell AJ, Thomas PG, Fersht AR (1987) Prediction of electrostatic effects of engineering of protein charges. Nature 330:86–88

Sugar IP, Neumann E (1984) Stochastic model for electric field-induced membrane pores. Electroporation. Biophys Chem 19:211–225

Sugar IP, Förster W, Neumann E (1987) Model of cell electroporation. Membrane electroporation, pore coalescence and percolation. Biophys Chem 26:321–335

Warshel A, Russell ST, Churg AK (1984) Macroscopic models for electrostatic interactions on proteins: Implications and applicability. Proc Natl Acad Sci USA 81:5785–5789